Gas-Liquid Mass Transfer with a Tangentially Moving Interface: Part I. Theory

CHARLES H. BYERS and C. JUDSON KING

University of California, Berkeley, California

A theoretical investigation has been made of the effect of a moving interface upon gas-liquid mass transfer, where the control of the mass transfer is entirely within the gas phase and where the control is distributed between the two phases. An analytical model is proposed for laminar interphase mass transfer in infinite media. Computer solutions have been obtained for gas-liquid mass transfer in confined phases. A cocurrent moving interface increases mass transfer coefficients over what they would be for the same flow rate without interfacial motion.

Many simple models have been suggested for the analysis of mass transfer between immiscible fluid phases. Most of these models neglect the effect of the fluid mechanics of one phase upon those of the other phase. For example, penetration or surface renewal models are often employed to describe liquid phase mass transfer near a free gas-liquid interface (*10, 22, 23,* etc.). Such models postulate no gradient of velocity in the liquid adjacent to the interface; this is generally a good assumption, since the viscosity of a gas is usually orders of magnitude less than that of a liquid. In situations where the liquid flows as a laminar layer over a solid surface, it is usually presumed that the free surface velocity for use in a penetration model is 3/2 the average velocity. Strictly speaking this is true only when there is zero drag at the interface. When there is a relatively high gas flow rate near the interface, the drag upon the interface may alter the interfacial velocity to an appreciable extent. As is shown below, this factor can assume importance.

Similarly, most models and correlations which have been proposed for gas phase resistance in gas-liquid contacting apparatus ignore the influence of the liquid surface velocity (*7, 19,* etc.). At least two theoretical papers have analyzed mass transfer near a moving surface (*1, 2*); however no concepts obtained from these works have been employed for the analysis of experimental mass transfer data. The influence of a moving interface is explored further in this paper and in Part II.

It is also common practice to ignore the interaction between the resistances to mass transfer offered by each of two contacting fluid phases, just as the interaction of the fluid mechanics is often ignored. The overall resistance to mass transfer is usually obtained from an equation of the form

$$\frac{1}{K_G a} = \frac{1}{k_G^* a} + \frac{H}{k_L^* a} \qquad (1)$$

The asterisks denote mass transfer coefficients measured in the absence or suppression of resistance in the other phase. Their use in Equation (1) implies that the value of each individual phase coefficient is unaltered by changes in the coefficient in the other phase. The use of a in Equation (1) implies that H and k_G/k_L are both constant across the entire contacting interface. The limitations of Equation (1) have been discussed by King (*12, 13*); its applicability to single cocurrent or countercurrent fluid exposures is explored further in the present work.

Although the ensuing discussion is carried out in the terminology of mass transfer, it applies as well to heat transfer between a gas and a liquid. Mass transfer considerations are restricted to low concentration levels and low net fluxes of mass. Presumably this restriction precludes any possibility of dynamic instabilities (Marangoni effect, etc.) entering the analysis. It is also assumed that the fluid interface is free in the sense that no surfactant layer is present to hamper flow. It is found in Part II of this work that this assumption is obeyed in many systems, but that for some cases of horizontal contacting, notably in aqueous systems, it is not obeyed.

Interphase heat and mass transfer in confined systems has been considered in a similar fashion by Nunge, Gill, and Stein (*16* to *18, 20*). The difference between the present work and theirs lies in the motion of the interface. The present work is concerned with situations where there is tangential interfacial motion, such as in direct fluid-fluid contacting. The analyses of Nunge, Gill, and Stein are concerned with situations where there is no interfacial motion, such as for heat exchange between fluids across a metallic dividing surface.

Flow Between Flat Plates

Consider a gas and a liquid in parallel, laminar, stratified flow between two parallel flat plates. The velocity profiles for this situation are shown in Figure 1. For generality it will be presumed that the flow rates of the gas and liquid streams can be set independently; this could occur if, for example, part or all of the impetus for liquid flow came from gravity. The two phases may be in cocurrent flow (U_{Gm} and U_{Lm} both positive) or countercurrent flow (U_{Gm} and U_{Lm} with different signs).

Charles H. Byers is with the University of Rochester, Rochester, New York.

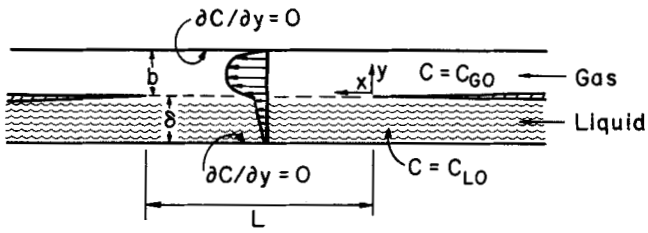

Fig. 1. Flow and interphase mass transfer between two flat plates.

The equation of motion may be solved for this two-dimensional case with the boundary conditions of zero velocity at $y = +b$ and $-\delta$, $U_G = U_L$ at $y = 0$, and $\mu_G(dU_G/dy) = \mu_L(dU_L/dy)$ at $y = 0$, giving

$$\frac{U_G}{U_{Gm}} = \frac{\frac{3}{2}\left(\frac{\delta\mu_G}{b\mu_L} + \frac{U_{Lm}}{U_{Gm}}\right)\left(1 - \frac{y^2}{b^2}\right) + 6\left(\frac{U_{Lm}}{U_{Gm}} - 1\right)\left(\frac{y^2}{b^2} - \frac{y}{b}\right)}{\left(\frac{\delta\mu_G}{b\mu_L} + 1\right)} \tag{2}$$

and

$$\frac{U_L}{U_{Lm}} = \frac{\frac{3}{2}\left(\frac{b\mu_L}{\delta\mu_G} + \frac{U_{Gm}}{U_{Lm}}\right)\left(1 - \frac{y^2}{\delta^2}\right) + 6\left(\frac{U_{Gm}}{U_{Lm}} - 1\right)\left(\frac{y^2}{\delta^2} + \frac{y}{\delta}\right)}{\left(\frac{b\mu_L}{\delta\mu_G} + 1\right)} \tag{3}$$

The ratio of the surface velocity to the average liquid velocity is

$$\frac{U_0}{U_{Lm}} = \frac{3}{2}\,\frac{\left(\frac{b\mu_L}{\delta\mu_G} + \frac{U_{Gm}}{U_{Lm}}\right)}{\left(\frac{b\mu_L}{\delta\mu_G} + 1\right)} \tag{4}$$

Thus the surface velocity is 3/2 the average liquid velocity only if $U_{Gm} = U_{Lm}$. For cocurrent flow with $U_{Gm} > U_{Lm}$, $U_0 > \frac{3}{2} U_{Lm}$; for cocurrent flow with $U_{Gm} < U_{Lm}$ or for countercurrent flow, $U_0 < \frac{3}{2} U_{Lm}$.

For many systems used in mass transfer μ_L is about fifty times μ_G. If $\delta = b$, $U_{Gm} = -U_{Lm}$ will correspond to $U_0 = 1.44\ U_{Lm}$, $U_{Gm} = 2U_{Lm}$ will correspond to $U_0 = 1.53\ U_{Gm}$, and $U_{Gm} = 10\ U_{Lm}$ will correspond to $U_0 = 1.76\ U_{Lm}$. The changes in the ratio of surface velocity to average liquid velocity become more severe as the gas phase becomes thinner in relation to the liquid. Thus for $b/\delta = 0.2$ and $\mu_L/\mu_G = 50$, the ratios for the three previous situations become 1.23, 1.64, and 2.00, respectively.

For the special case of true horizontal two-phase flow, the pressure drop serves as the sole impetus of flow for both gas and liquid. A derivation similar to that given by Bird et al. (3) yields

$$\frac{U_{Gm}}{U_{Lm}} = \frac{4 + \frac{b\mu_L}{\delta\mu_G} + 3\frac{\delta}{b}}{4\frac{\delta}{b} + \frac{\delta^2\mu_G}{b^2\mu_L} + 3} \tag{5}$$

and

$$\frac{U_0}{U_{Lm}} = \frac{6\left(1 + \frac{\delta}{b}\right)}{4\frac{\delta}{b} + \frac{\delta^2\mu_G}{b^2\mu_L} + 3} \tag{6}$$

The interfacial velocity is 3/2 the average liquid velocity only if $\delta^2\mu_G = b^2\mu_L$. If $\delta^2\mu_G > b^2\mu_L$, $U_0 < \frac{3}{2} U_{Lm}$; and if $\delta^2\mu_G < b^2\mu_L$, $U_0 > \frac{3}{2} U_{Lm}$. For phases of equal thickness with $\mu_L = 50\ \mu_G$, $U_0 = 1.71\ U_{Lm}$.

PHASES OF INFINITE EXTENT

For mass transfer during brief exposures of a gas and a liquid in confined flow, it is permissible to consider only the region very near the interface and to neglect the effect of the confining walls upon the mass transfer process. The following sections will consider mass transfer between gas and liquid phases which are in fully developed cocurrent parallel flow and are infinite in extent. Cases considered include gas phase-controlled mass transfer, liquid phase-controlled mass transfer, and the general interphase case where the resistances of both phases are important. Even though the models consider phases of infinite extent, they are applicable to many cases of confined flow. The extent to which unconfined models are applicable to confined cases is discussed below.

Gas Phase-Controlled Mass Transfer

The velocity profile near the gas-liquid interface may be taken to be linear for cases of brief exposures where the concentration changes due to mass transfer do not penetrate the gas deeply. A general model for the mass transfer process in this situation is shown in Figure 2.

In this case the velocity profile is

$$U_G = U_0 + ay \tag{7}$$

Therefore the diffusive transport equation reduces to

$$(U_0 + ay)\frac{\partial c_A}{\partial x} = D_G \frac{\partial^2 c_A}{\partial y^2} \tag{8}$$

with the boundary conditions

$$\begin{array}{lll} \text{at} & y = 0 & c_A = c_{AS} \\ & x = 0 & c_A = c_{A0} \\ & y = \infty & c_A = c_{A0} \end{array} \tag{9}$$

This problem has been solved by Beek and Bakker (2) by Laplace transformation. Two asymptotic solutions were found for the local mass transfer coefficients based upon the initial driving force. For short exposures ($a^2D_G\,x/U_0^3 << 1$), the solution is

$$k_{CG}\left(\frac{x}{U_0 D_G}\right)^{1/2} = \frac{1}{\sqrt{\pi}} + \frac{1}{4}\left(\frac{a^2 D_G x}{U_0^3}\right)^{1/2} \tag{10}$$

while for long exposures ($a^2D_G\,x/U_0^3 >> 1$)

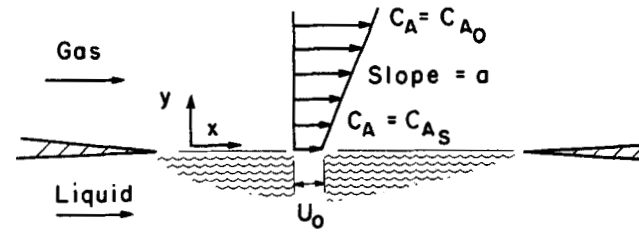

Fig. 2. The Beek and Bakker model for mass transfer to an infinite medium with an interfacial velocity.

$$k_{CG}\left(\frac{x}{U_0D_G}\right)^{1/2} = 0.538\left(\frac{a^2D_Gx}{U_0^3}\right)^{1/6}\left[1 + 0.375\left(\frac{U_0^3}{a^2D_Gx}\right)^{1/3}\right] \quad (11)$$

Beek and Bakker used interpolation to approximate the solution in the intermediate region (a^2D_Gx/U_0^3 on the order of the 1). An exact solution in this region is desirable because it must be used in estimating average mass transfer coefficients for all but the shortest exposures. A numerical digital computer solution was made of the problem by using a Crank-Nickolson six-point implicit formula to approximate the parabolic partial differential equation. It was necessary to calculate local mass transfer coefficients by means of a numerical differentiation of the concentration profile at the interface. An unsymmetrical five-point formula provided the necessary accuracy. It was found that the correct solution in the intermediate region is the one shown in Figure 3 as a solid line. The hatched curves are the asymptotic solutions [Equations (10) and (11)]. The exact solution lies below the two asymptotic solutions rather than between them, as was originally estimated by Beek and Bakker (compare Figure 3 of reference 2).

For short exposures, where the slope in the velocity profile becomes unimportant compared to the interfacial velocity, the solution approaches the penetration model:

$$k_{CG}\left(\frac{x}{U_0D_G}\right)^{1/2} = \frac{1}{\sqrt{\pi}} \quad (12)$$

For higher values of the abscissa, where the interfacial velocity is small compared with velocities a short distance away in the gas, the solution approaches the Levêque model for transfer from a stagnant surface into a fluid with a linear velocity profile:

$$k_{CG}\left(\frac{x}{U_0D_G}\right)^{1/2} = 0.538\left(\frac{a^2D_Gx}{U_0^3}\right)^{1/6} \quad (13)$$

In the intermediate region, however, the mass transfer coefficient is higher than predicted by either of these two limiting models. Near an abscissa of 1.0 both limiting models are in error by 30%. The physical basis for this behavior is clear enough: The penetration model allows for the interfacial velocity, but neglects the increased convective removal of mass resulting from the increase in velocity with distance away from the surface. The Levêque model allows for the increase in velocity with distance away from the interface, but neglects the convective removal of mass resulting from the finite velocity at the interface itself. Therefore, it is logical that both the penetration and Levêque models underestimate the mass transfer coefficient.

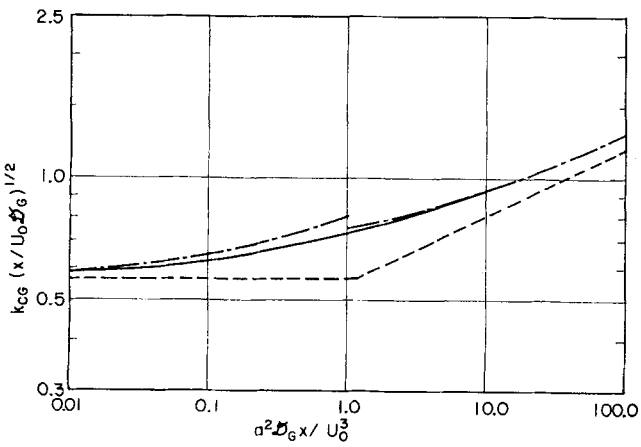

Fig. 3. Solution for mass transfer to an infinite medium with an interfacial velocity: ——— — ——— asymptotic solutions, ——— exact solution, — — — limiting solutions.

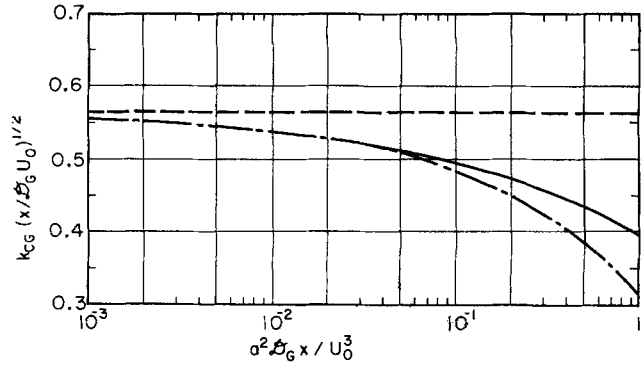

Fig. 4. Solution for mass transfer to a phase with a negative slope in the velocity profile: ——— — ——— asymptotic solution, ——— exact solution, — — — penetration model.

The Beek and Bakker model assumes that the slope of the velocity profile in the medium in question is positive. There are a number of situations where the slope is negative, and therefore it is of considerable interest to carry through such a solution. Strictly speaking, one may not postulate an infinite phase for the case of a negative slope of the velocity profile, since a flow reversal must occur at some distance from the interface. This in turn would necessitate the provision of initial concentrations at both ends of the exposure (at $x = 0$ and $x = L$ in Figure 2). However, if the value of a^2D_Gx/U_0^3 is sufficiently small, the solution should not be sensitive to the flow reversal. If we carry out the solution for a short-exposure asymptote, the result is

$$k_{CG}\left(\frac{x}{U_0D_G}\right)^{1/2} = \frac{1}{\sqrt{\pi}} - \frac{1}{4}\left(\frac{a^2D_Gx}{U_0^3}\right)^{1/2} \quad (14)$$

For any physically significant case the long-exposure asymptote with Equation (9) as boundary conditions is meaningless. It is evident that Equation (14) is a mirror image of Equation (10) about the penetration solution. Equation (14) is shown as the hatched line in Figure 4. The dotted line is the penetration model, while the solid line is the exact solution of this problem, which was carried out numerically by computer methods.

The solution for a negative velocity gradient allows some qualitative remarks concerning two important situations. In most cases where a gas and a liquid are in cocurrent motion, the gas is moving sufficiently quickly to cause some drag upon the liquid interface, which in turn causes a small negative slope in the liquid phase velocity. With this solution we are able to say that if the value of a^2D_Lx/U_0^3 is less than 10^{-3}, the penetration theory is obeyed to within 2%. The other important case is when a gas and a liquid are in countercurrent flow. Here there will be a negative slope in the velocity profile in gas at the interface. While Equation (14) is invalid for most countercurrent problems, it is interesting that the solution does predict that the negative slope causes a decrease in the mass transfer coefficient. This fact was confirmed experimentally in Part II of the present work. Equation (14) could not be applied directly in that study, since the flow reversal played an important role in all the experiments.

Liquid Phase-Controlled Mass Transfer

Strictly speaking, a model similar to that developed for the gas phase would apply to the mass transfer resistance

of an adjacent liquid. However, since the drag of the gas on the liquid is relatively small and since liquid diffusivities are low, one is almost invariably located on the penetration asymptote of Figure 3. Hence, no features of the liquid velocity profile need be considered for mass transfer purposes aside from the velocity of the interface itself. If a liquid with a constant velocity U_0 is exposed to a medium which imparts to its interface a constant concentration different from that in the entering bulk, the transport equation reduces to

$$U_0 \frac{\partial c_A}{\partial x} = D_L \frac{\partial^2 c_A}{\partial y^2} \tag{15}$$

The local mass transfer coefficient based upon the initial driving force will be

$$k_{CL} = (D_L U_0/\pi x)^{1/2} \tag{16}$$

For flow between parallel plates U_0 would be calculated by means of Equation (3). This form of the penetration model has been shown to be appropriate in many liquid phase-controlled situations (*8, 21, 23,* etc.).

Interphase Mass Transfer

A model for interphase mass transfer in fully developed flow is shown in Figure 5. Two infinite phases—a gas with an interfacial velocity U_0 and a velocity profile with a constant slope a, and a liquid with constant velocity U_0 —are contacted for a length L. The convective transport equation for the gas phase is the same as Equation (8), while in the liquid phase the equation is the same as Equation (15). The boundary conditions are

$$\left.\begin{array}{lll} \text{At} \quad x = 0 & y > 0 & c_G = c_{G0} \\ x = 0 & y < 0 & c_L = c_{L0} \end{array}\right\} \tag{17}$$

$$\left.\begin{array}{lll} \text{At} \quad y = +\infty & & c_G = c_{G0} \\ y = -\infty & & c_L = c_{L0} \end{array}\right\} \tag{18}$$

The interfacial conditions at $y = 0$ are

$$D_G \frac{\partial c_G}{\partial y} = D_L \frac{\partial c_L}{\partial y} \tag{19}$$

$$c_G = \mathcal{H}\, c_L \tag{20}$$

The first equation is the continuity of fluxes across the interface, while the second is the assumption of Henry's law as the equilibrium interfacial condition. The constant $\mathcal{H}$ is dimensionless (H/RT).

The problem is solved by Laplace transformation. In the Laplace domain the liquid phase solution is the solution for penetration into a stream with constant velocity

$$\bar{c}_L = \frac{c_{L0}}{s} + \Lambda \exp\left(y \sqrt{\frac{U_0 s}{D_L}} \right) \tag{21}$$

$$\frac{d\bar{c}_L}{dy} = \Lambda \sqrt{\frac{U_0 s}{D_L}} \exp\left(y \sqrt{\frac{U_0 s}{D_L}} \right) \tag{22}$$

where s is the Laplace transform variable and Λ is a constant to be determined by the application of the interfacial conditions.

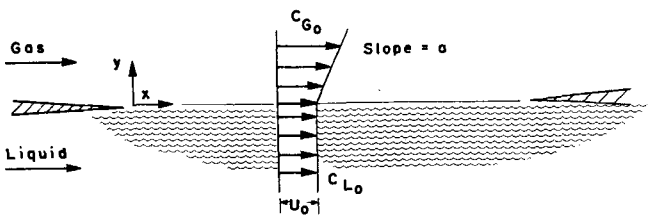

Fig. 5. Model for interphase mass transfer with control distributed between gas and liquid.

The gas phase solution is carried out by the same method as the solution of Beek and Bakker (*2, 5*). The solution in the Laplace domain to this portion of the problem is

$$\bar{c}_G = \frac{c_{G0}}{s} + \theta \left(1 + \frac{a}{U_0} y \right)^{1/2} K_{1/3}\left[\frac{2}{3} \left(\frac{U_0^3}{a^2 D_G} \right)^{1/2} s^{1/2} \left(1 + \frac{a}{U_0} y \right)^{3/2} \right] \tag{23}$$

$$\frac{d\bar{c}_G}{dy} = -\theta \frac{a}{U_0} \left(1 + \frac{a}{U_0} y \right) \left(\frac{U_0^3}{a^2 D_G} \right)^{1/2} s^{1/2} K_{-2/3}\left[\frac{2}{3} \left(\frac{U_0^3}{a^2 D_G} \right)^{1/2} \cdot s^{1/2} \left(1 + \frac{a}{U_0} y \right)^{3/2} \right] \tag{24}$$

where θ is a constant. The two constants Λ and θ are obtained by the simultaneous application of the two interfacial conditions [Equations (19) and (20)] to the solutions in the Laplace domain.

$$\Lambda = \frac{\Delta c}{s} \frac{\mathcal{H}\sigma \left[K_{-2/3}\left(\frac{2}{3} \zeta s^{1/2} \right) \right]}{\mathcal{H}\sigma K_{-2/3}\left(\frac{2}{3} \zeta s^{1/2} \right) + K_{1/3}\left(\frac{2}{3} \zeta s^{1/2} \right)} \tag{25}$$

$$\theta = -\frac{\Delta c}{s} \left[\frac{\mathcal{H}}{\mathcal{H}\sigma K_{-2/3}\left(\frac{2}{3} \zeta s^{1/2} \right) + K_{1/3}\left(\frac{2}{3} \zeta s^{1/2} \right)} \right] \tag{26}$$

where

$$\sigma = (D_G/D_L)^{1/2} \qquad \zeta = \left(\frac{U_0^3}{a^2 D_G} \right)^{1/2}$$

$$\Delta c = \frac{c_{G0}}{\mathcal{H}} - c_{L0} \tag{27}$$

and

$$z = \frac{2}{3} \zeta s^{1/2} \tag{28}$$

It is obvious that concentration profiles would be quite difficult to generate. As a result only a solution for the mass transfer coefficient is sought. The local overall mass transfer coefficient based on the initial driving force is defined in the Laplace domain as

$$\bar{K}_{CG} = -\frac{D_G}{\Delta c} \frac{d\bar{c}_G}{dy} \qquad y = 0 \tag{29}$$

and is found to be

$$\bar{K}_{CG} = \frac{2\mathcal{H} U_0^2}{3 z a} \left(\frac{K_{-2/3}(z)}{\sigma \mathcal{H} (K_{-2/3}(z)) + K_{1/3}(z)} \right) \tag{30}$$

No simple general solution is available for this problem. However it is possible to find asymptotic solutions for short and long exposures. For large values of z, the following simple form may be given to the Bessel's function of the second kind:

$$K_n(x) = \sqrt{\frac{\pi}{2x}} e^{-x} [R_n + S_n] \tag{31}$$

where R_n and S_n are series in n and x given by Carslaw and Jaeger (6). If this approximation is included in the solution and the binomial in the denominator is expanded in a series, the result is

$$\bar{K}_{CG} = \frac{\gamma}{\alpha}\left[\left(\frac{1}{z}\right) + \left(\frac{\beta}{\alpha} + \frac{7}{72}\right)\left(\frac{1}{z}\right)^2 + \left(\frac{\beta^2}{\alpha^2} + \frac{455}{10{,}368} + \frac{7}{72}\,\frac{\beta}{\alpha}\right)\left(\frac{1}{z}\right)^3 + \ldots.\right] \quad (32)$$

where

$$\left.\begin{aligned} \gamma &= 2\,\mathcal{H}U_0^2/3\,a \\ \alpha &= \sigma\mathcal{H} + 1 \\ \beta &= \frac{5 - 7(\sigma\mathcal{H} + 1)}{72} \end{aligned}\right\} \quad (33)$$

This series may be inverted term by term. The overall mass transfer coefficient based upon the gas phase is

$$K_{CG} = \frac{\gamma}{\alpha}\left(\frac{3}{2\,\zeta\sqrt{\pi x}} + \frac{9}{4\zeta^2}\left(\frac{\beta}{\alpha} + \frac{7}{72}\right) + \ldots.\right) \quad (34)$$

Rearrangement gives

$$K_{CG}\left(\frac{x}{U_0 D_G}\right)^{1/2} = \frac{\mathcal{H}\,\zeta}{\sigma\mathcal{H} + 1}\left[\frac{1}{\zeta\sqrt{\pi}} + \frac{6\,x^{1/2}}{4\,\zeta^2}\left(\frac{5 - 7\sigma\mathcal{H}}{(\sigma\mathcal{H} + 1)72} + \frac{7}{72}\right) + \ldots\right] \quad (35)$$

The solution for low values of z is not quite as satisfactory. For small values of z

$$K_p(x) = 2^{p-1}\,(p-1)!\,x^{-p} \quad (36)$$

For this case Equation (30) becomes

$$\bar{K}_{CG} \simeq \frac{\gamma}{z}\left(\frac{1}{\sigma\mathcal{H} + F\,z^{1/3}}\right) \quad (37)$$

where

$$F = 2^{-1/3}(-2/3)!/(-1/3)! \quad (38)$$

A solution is difficult in this case so that we seek a solution only for the situation where

$$\sigma\mathcal{H} > F\,z^{1/3}$$

Let

$$\tau = \frac{\sigma\mathcal{H}}{F}$$

Then if

$$z^{1/3}/\tau << 1$$

$$\bar{K}_{CG} = (1 - z^{1/3}/\tau + z^{2/3}/\tau \ldots.) \quad (39)$$

The solution is inverted and rearranged. Finally the coefficients are evaluated, resulting in

$$K_{CG}\left(\frac{x}{D_G U_0}\right)^{1/2} = \frac{1}{\sigma\mathcal{H}}\left[\frac{1}{\sqrt{\pi}} - \frac{0.515}{\sigma\mathcal{H}\left(\frac{a^2 D_G x}{U_0^3}\right)^{1/6}} + \frac{0.343}{(\sigma\mathcal{H})^2\left(\frac{a^2 D_G x}{U_0^3}\right)^{1/3}} + \ldots\right] \quad (40)$$

The results of this solution are shown graphically in Figure 6. A presentation of $K_{CG}(x/U_0 D_G)^{1/2}$ as a function of $a^2 D_G x/U_0^3$ is made for different values of the parameter $\sigma\mathcal{H}$. The solid line represents the analytical solution, while the dotted line shows results of a computer solution of the same problem in the regions where the analytic solution is not valid. This computer solution is discussed in detail elsewhere (5).

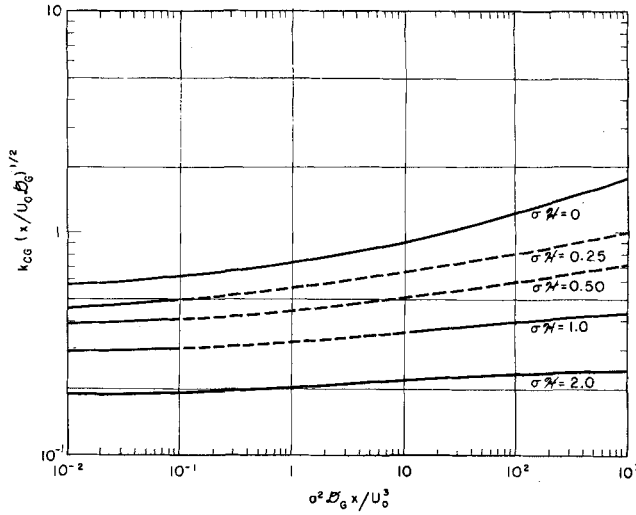

Fig. 6. Interphase mass transfer solution for unbounded media: —— analytic solution, — — — computer solution.

King (12) has shown that the addition of resistances principle [Equation (1)] should be closely obeyed for cocurrent flow. This will be particularly true to the extent that the independently measured individual phase mass transfer coefficients tend to vary with the same power of the distance since the start of an exposure. The addition of resistances principle should therefore be effective for the prediction of the results shown in Figure 6, since for liquid phase-controlled mass transfer the coefficient varies as $x^{-1/2}$, while for gas phase-controlled mass transfer, the coefficient varies as $x^{-1/2}$ for very short times with the exponent increasing toward $-1/3$ at longer times.

Addition of resistances for the independently measured local coefficients at all points yields

$$K_{CG}\left(\frac{x}{D_G U_0}\right)^{1/2} = \frac{k_{CG}\left(\frac{x}{D_G U_0}\right)^{1/2}}{1 + \sqrt{\pi}\,\sigma\mathcal{H}\,k_{CG}\left(\frac{x}{D_G U_0}\right)^{1/2}} \quad (41)$$

The penetration model is employed for the liquid phase, and the gas phase mass transfer group $k_{CG}\left(\frac{x}{D_G U_0}\right)^{1/2}$ is taken from Figure 3.

The solution using the additivity of resistances was compared with the analytical solution where it is applicable and the computer solution in the remainder of the region. It was found that the deviations of the additivity solution were greatest in the region where $\sigma\mathcal{H}$ is near unity, that is, where control is evenly divided between phases. Also the deviation tends to increase as $a^2 D_G x/U_0^3$ increases, but the maximum deviation is less than 2% for any reasonable value of the length group ($<$100,000). The use of the addition of resistances with average coefficients is similarly effective.

CONFINED PHASES

Interphase mass transfer situations generally involve confined fluid phases; hence it is important to analyze the rates of mass transfer which are to be expected in confined flows. Such analyses are particularly needed for the interpretation of the experimental measurements reported in Part II. The prediction of mass transfer coefficients is simpler for fluids of infinite extent. It is therefore important to compare the unbounded models with the corresponding confined flow solutions in order to

identify the degree of equilibration or duration of surface exposure for which the former are valid.

Mass Transfer Controlled by a Single Phase

The hydrodynamic simplicity of laminar flow in a circular tube made the prediction of mass and heat transfer coefficients for that case a relatively simple task. Since the original solution by Graetz (9) for uniform wall temperature or concentrations, there have been several solutions made of this problem for various boundary conditions. Mass transfer to laminar flow between two infinitely wide flat plates is similar to the Graetz problem. The constants generated by this solution are of course somewhat different from those in the original Graetz solution.

The problem of mass transfer to a stream flowing between two flat plates has been solved by Butler and Plewes (4) for the case of a constant solute concentration at one wall, different from that in the entering fluid stream, and a zero flux at the other wall. A modification of their velocity profile is needed for the present study. The wall at which the mass transfer takes place is a fluid interface which is in motion with a velocity U_0 relative to the fixed wall. The physical situation is illustrated in Figure 7. The fluid enters with a solute concentration C_{A0} and is contacted with an immiscible fluid which holds the concentration at the interface constant at C_{AS}. The velocity profile may be expressed as

$$U_G = U_0 + (6U_{Gm} - 4U_0)\, y/b + (3U_0 - 6U_{Gm}) \left(\frac{y}{b}\right)^2 \tag{42}$$

The profile is also applicable to the liquid, in which case U_L is expressed as a function of U_0, U_{Lm}, and y/δ. The transport equation for this case may be written nondimensionally as

$$[1 + (6V - 4)Y + (3 - 6V)Y^2] \frac{\partial C}{\partial X} = \frac{\partial^2 C}{\partial Y^2} \tag{43}$$

The boundary conditions are

$$\begin{array}{ll} X = 0 & C = 0 \\ Y = 0 & C = 1 \\ Y = 1 & \partial C/\partial Y = 0 \end{array} \tag{44}$$

The velocity profile is parabolic and the problem could be solved by a method of separation of variables in the same way as Butler and Plewes solved for the case of zero interfacial motion. The present situation must be solved for a wide range of values of the parameter V. As a result, the generation of constants was found to be impractical, and the equation was solved directly on the computer for seven values of the parameter $V = U_m/U_0$. These range from 0.5 to 100, the latter figure being essentially equivalent to the solution of Butler and Plewes. Equation (43) is a parabolic partial differential equation and therefore may be put in finite-difference form by the application of the Crank-Nicholson six-point implicit formula. The resulting tridiagonal matrix may be solved directly by a Thomas method (14) and corrected by means of a Gauss-Seidell procedure with a successive overrelaxation factor

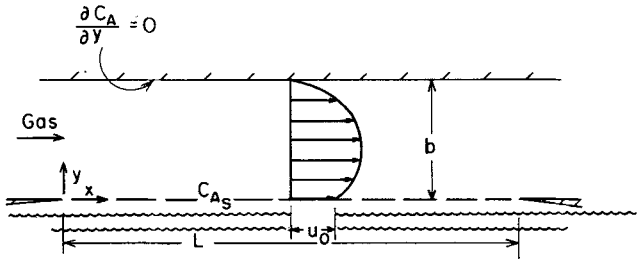

Fig. 7. Mass transfer to a fluid in laminar flow between two parallel walls, one of which is in cocurrent motion.

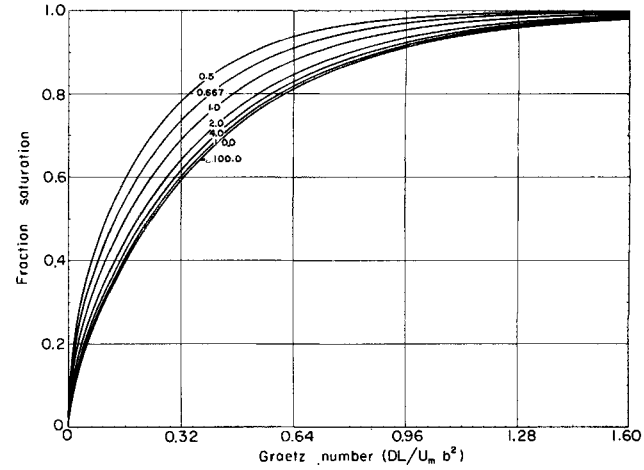

Fig. 8. Mean fraction saturation as a function of the Graetz number for different values of the parameter U_m/U_0.

used. A listing of the Fortran programs written for this solution along with all the other programs mentioned in the present discussion may be found elsewhere (5).

The results were given directly in the form of graphs on the digital plotter. Figure 8 shows the average (cup mixing) fraction saturation $[(C_A - C_{A0})/(C_{AS} - C_{A0})]_{AV}$, as a function of the Graetz number $D_G x/U_m b^2$ for the seven values of the parameter U_m/U_0 which were considered. The solution was verified by comparison with the two pertinent analytical solutions available. The solution by Butler and Plewes almost perfectly matched the solution for the highest value of U_m/U_0 (100) over the entire range for which the former is valid. Pigford (11) has solved for the case of liquid flow down a plane, where U_m/U_0 is 2/3. Again in this case the present solution almost perfectly matched the earlier solution from a fraction saturation of 0.20 to 1.00. At values of the average fraction saturation below 0.2, insufficient terms are available for the analytical solution.

The effect of the interfacial velocity upon the mass transfer process is quite clearly shown in Figure 8. For a given system, if the average velocity of the gas phase U_m is kept constant and the interfacial velocity U_0 is al-

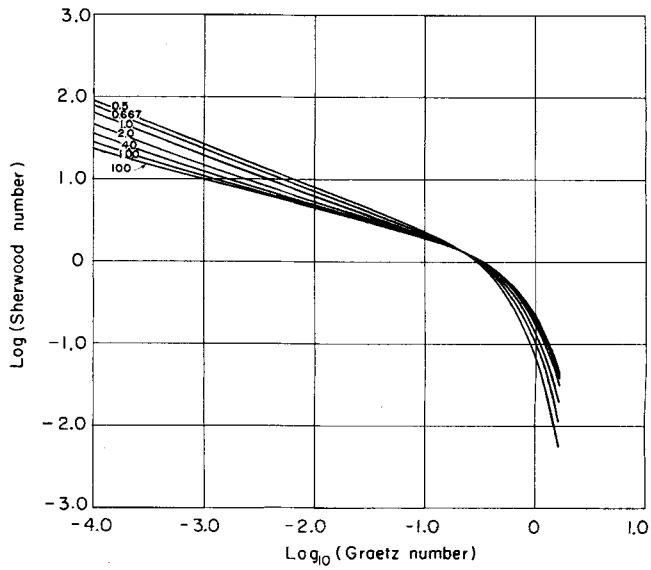

Fig. 9. A logarithmic representation of the local Sherwood number as a function of the Graetz number for different values of the parameter U_m/U_0.

lowed to increase from zero to a high value, one moves vertically upward on the graph. It is obvious that there is a considerable increase in the mass transfer coefficient merely because of the fact that the interface is in motion. For example at a Graetz number of 0.32, the average fraction saturation corresponding to no interfacial motion ($V = 100$) is 0.58, while for $V = 0.5$ this increases to 0.78.

The local Sherwood number (Nusselt number for mass transfer) based upon the initial driving force was computed, using an unsymmetrical five-point formula to estimate the local mass transfer flux. For very short exposures numerically estimated derivatives are inaccurate, and therefore only values of the Sherwood number for values of the Graetz number greater than 10^{-4} are shown in Figure 9. This figure is a logarithmic plot of the local Sherwood number as a function of the Graetz number, for the same seven values of the velocity parameter. The curves cross at a Graetz number of about 0.2, since at higher interfacial velocities saturation is achieved at a lower Graetz number. The fact that the curves all cross at one point appears to be a coincidence.

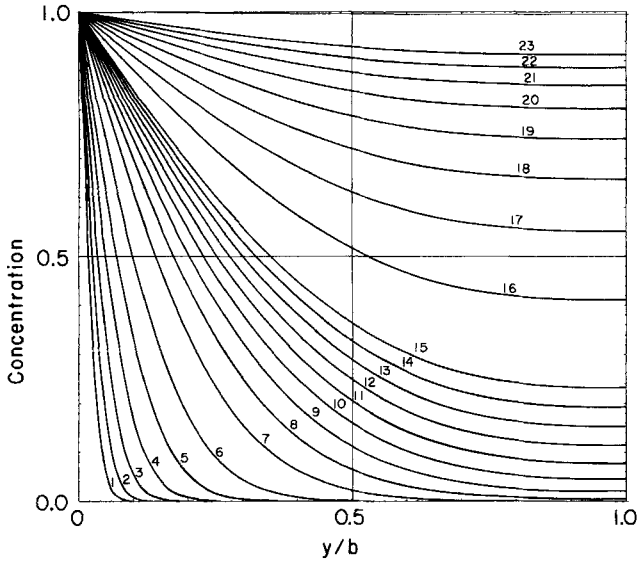

Fig. 10. Concentration ($C_A - C_{A0}/C_{AS} - C_{A0}$) as a function of distance from the interface with U_m/U_0 equal to 2/3 for the values of the Graetz numbers listed below.

No. of curve	Graetz No.
1	0.0005
2	0.001
3	0.002
4	0.004
5	0.008
6	0.016
7	0.032
8	0.048
9	0.064
10	0.080
11	0.096
12	0.112
13	0.128
14	0.144
15	0.16
16	0.24
17	0.32
18	0.40
19	0.48
20	0.56
21	0.64
22	0.72
23	0.80

Finally, concentration profiles were generated for all of the values of U_m/U_0 mentioned above. Figure 10 is a typical set of profiles for $U_m/U_0 = 2/3$. The profiles for the other cases are reported elsewhere (5). The dimensionless concentration C is plotted as a function of the fractional distance from the interface with the Graetz number as a parameter. This series of profiles is of particular interest since it is the solution to mass transfer into a liquid flowing down a plane where there is no drag upon the interface. For this case, it is normal to use the penetration model in the estimation of the mass transfer coefficients and concentration profiles. When the exact solution is compared with the penetration model, it is found that the latter is a close approximation up to an average fraction saturation of about 0.60 for estimating the average mass transfer coefficient. The concentration profiles are in agreement up to a Graetz number of 0.04.

Another comparison which is of interest is between the infinite phase model with a positive slope in velocity and the confined flow solution. For this comparison a value of U_m/U_0 of 2.0 was chosen for the confined case. The concentration profiles coincide only up to a Graetz number of 0.01 (average fraction saturation of 0.125). On the other hand, the average mass transfer coefficient was valid to within 10% up to a Graetz number of 0.2, which represents an average fraction saturation of about 50%.

Interphase Mass Transfer

When a third component passes from a solvent to an inert carrier gas, the resistance to mass transfer is in general distributed between the two phases. In the analytic solution to the unbounded problem it was found that the degree of control which is resident in either phase is dependent upon the parameter $(D_G/D_L)^{1/2}(H/RT)$. In the confined flow case this group serves the same purpose. The convective transport equation was solved for two different cases of confined interphase mass transfer. The experimental study which accompanied this theoretical work had the geometry shown in Figure 1. Therefore, the first solution involves transfer between two confined phases, both of which have parabolic profiles. The partial differential equations for both phases may be put into finite-difference form by means of a Crank-Nicholson formula. Henry's law is used to describe the equilibrium relationship at the interface. This assumption, along with the equality of fluxes [Equations (19) and (20)] is used to define the connection between the two phases at the interface. The resulting tridiagonal matrix is solved by the usual techniques. In the case where both phases have parabolic profiles in velocity, three independent parameters are necessary to define the problem. Therefore, a general solution is not pragmatic. The experimentally important cases were solved with this model, while the general solution was carried out with a simplified velocity profile. The three independent parameters necessary to define each case may be reduced by one if a constant velocity equal to the interfacial velocity is assumed in the liquid phase. Since the effect of the mass transfer penetrates to only a small fraction of the total liquid depth, this assumption is almost always applicable. The two remaining independent parameters are the velocity parameter U_m/U_0 and the control parameter $(D_G/D_L)^{1/2}$ (H/RT). This problem was solved for five different values of the control parameter (5, 2, 1, 0.5, and 0.25). Figures 11 and 12 are the results for $\sigma H = 1$. The other results are also available (5). Figure 11 presents the local Sherwood number based upon the initial driving force as a function of the Graetz number. Figure 12 shows the average fraction saturation as a function of the Graetz number.

This solution provides an opportunity to compare the predictions of the addition of the resistances principle with the exact solution for a cocurrent laminar confined

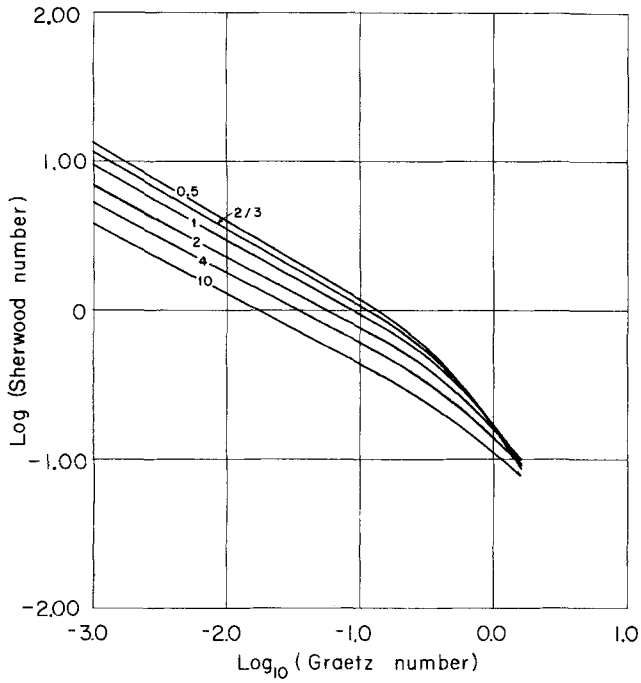

Fig. 11. Local Sherwood numbers as a function of the Graetz number for different values of the parameter U_m/U_0 with $\sigma\mathcal{H} = 1.0$ for a model with a confined gas and an infinite liquid.

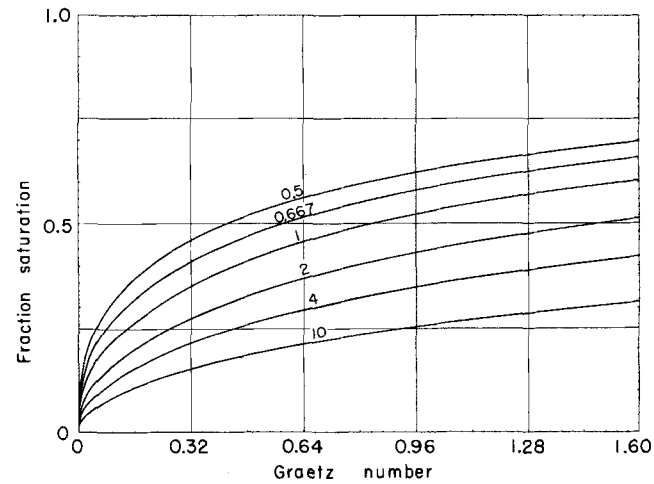

Fig. 12. Average fraction saturation as a function of the Graetz number for different values of the parameter U_m/U_0 with $\sigma\mathcal{H} = 1.0$ for a model with a confined gas and an infinite liquid.

flow case. Most other such comparisons have been made for models in which there are infinite media (*12, 13*, etc.). One comparison which does exist for confined media pictures a countercurrent turbulent confined phase to which the film model is applied (*15*); another considers two confined streams in cylindrical (*17*) or flat plate (*18*) geometry with no interfacial motion. In the present solution it is interesting to ascertain whether the effect of the penetration of the mass transfer to the wall may be properly predicted by the addition of the two independently measured individual resistances. For the gas phase resistance the confined flow case with a moving interface is used, while the penetration model is chosen to describe the liquid phase behavior. The addition of the resistances principle was applied to predict local and average Sherwood numbers for the interphase mass transfer case. For the sake of comparison, values of $\sigma\mathcal{H}$ of 1 and a velocity parameter of $V = 4$ were chosen. These probably represent the most severe test of the addition of the resistances principle. The ratio of the predicted and actual Sherwood numbers is shown in Figure 13. The solid curve represents the comparison of local Sherwood numbers as a function of the Graetz number, with the Sherwood numbers based upon the initial driving force ($\mathcal{H}c_{L0} - c_{G0}$). At low Graetz numbers the situation reduces to the problem previously analyzed for phases of infinite extent. As has already been noted, the addition principle works well in this range. At Graetz numbers above 0.5 the addition of resistances prediction becomes increasingly erroneous. In this range the gas phase approaches saturation in the gas phase-controlled case; this necessarily causes the individual gas phase Sherwood number based on the initial driving force to drop toward zero and causes the predicted overall coefficient to follow. In the interphase case the gas phase is less saturated at a given Graetz number and the true overall coefficient remains high.

Because of this behavior one might expect that the addition principle would work better if applied to local Sherwood numbers based upon the local driving force. Such a comparison is also given in Figure 13, with cup-mixing concentrations used as driving forces. In this case the addition principle predicts too high a mass transfer coefficient at high Graetz numbers. This is at least partially caused by the fact that the local driving force approaches zero at lower Graetz numbers for the individual gas phase resistance than for the overall resistance to mass transfer.

Also shown in Figure 13 are comparisons for predicted and actual values of the average Sherwood group. The average Sherwood group based upon the log mean driving force exhibits a deviation from the addition principle which is similar to that for the local Sherwood number based on the local driving force. The average Sherwood group based on the initial driving force, on the other hand, shows agreement with the addition principle to a Graetz number of 2. This form of Sherwood group weights the initial mass transfer highly; it has already been shown that the initial mass transfer follows a penetration model

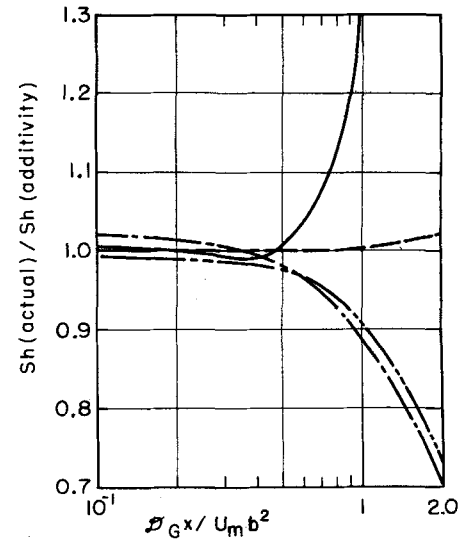

Fig. 13. A comparison of the exact solution for interphase mass transfer from an infinite liquid phase to a confined gas phase with the results of the addition of resistances model for U_m/U_0 equal to 4 and $\sigma\mathcal{H} = 1.0$. ——— local Sherwood number based on initial driving force, — — — average Sherwood number based on initial driving force, ——— — ——— local Sherwood number based on local driving force, ——— — — ——— average Sherwood number based on logarithmic mean driving force.

in both phases and thus gives average overall coefficients which agree well with the addition principle. Thus, the preferred form of application of the addition principle is that corresponding to the dashed curve in Figure 13:

$$\frac{1}{K_{CG}a} = \frac{1}{k^*_{CG}a} + \frac{\mathcal{H}}{k^*_{CL}a} \qquad (45)$$

where the mass transfer coefficients are based on the initial driving force and are averaged over the exposure.

CONCLUSIONS

1. In many instances of gas-liquid mass transfer it is important to allow for the effects of the interaction of the fluid mechanics of the contacting phases.
2. In most cases of laminar gas-liquid contacting the liquid phase will follow a penetration model closely, but the surface velocity to be used in the model may be greater or less than 3/2 the average velocity.
3. Gas phase mass transfer in cocurrent, laminar, gas-liquid flow is influenced by the interfacial velocity. For well-developed flow with phases of infinite extent, the mass transfer coefficient is given by Figure 3 and is greater than predicted by either the Levêque or penetration models.
4. The effect of confining walls on cocurrent, laminar gas-liquid mass transfer causes mass transfer coefficients to be less than those given by Figure 3 for the gas and less than those given by the penetration model for the liquid. These effects become important above 50% equilibration of either phase.
5. The addition of the resistances principle should work well for gas and liquid phases of infinite extent (brief exposures) in cocurrent, laminar flow. For confined phases the most effective form of the addition principle is that given by Equation (45).

ACKNOWLEDGMENT

This work was performed in the Lawrence Radiation Laboratory under the auspices of the U.S. Atomic Energy Commission.

NOTATION

a = slope of the velocity of a phase at the interface, sec.$^{-1}$
a = area of mass transfer exposure, sq.cm.
b = thickness of gas phase, cm.
c = concentration of a transferring component in a phase, $\Delta c = \mathcal{H}c_{L0} - c_{G0}$, g.-moles/cc.
C = dimensionless concentration, $(C_A - C_{A0})/(C_{AS} - C_{A0})$
D = diffusion coefficient, sq.cm./sec.
F = constant as defined in Equation (38)
H = Henry's law constant, (atm.)(cc.)/g.-mole
$\mathcal{H}$ = dimensionless Henry's law constant, H/RT
k_c = local mass transfer coefficient based upon the initial concentration driving force, cm./sec.
K = Bessel function of the second kind
K_c = overall mass transfer coefficient based upon the initial concentration driving force, cm./sec.
L = length of exposure, cm.
n = index of series
p = order of the Bessel function
R = universal gas constant, (atm.)(cc.)/(g.-mole)(°K.)
R_n = remainder series as defined in reference 6
s = Laplace transform variable
S_n = remainder series as defined in reference 6
T = absolute temperature, °K.
U_0 = interfacial velocity, cm./sec.
V = velocity parameter, U_m/U_0
x = distance from start of exposure, cm.
X = $D_G x/U_0 b^2$
y = direction and distance perpendicular to the interface, cm.
Y = y/b
z = $2/3\ \zeta\ s^{1/2}$

Greek Letters

α = $\sigma\mathcal{H} + 1$
β = $[5 - 7(\sigma\mathcal{H} + 1)]/72$
γ = $2\mathcal{H}\ U_0^2/3a$
δ = thickness of the liquid phase, cm.
ζ = $(U_0^3/a^2 D_G)^{1/2}$
θ = constant as defined in Equation (26)
Λ = constant as defined in Equation (25)
μ = viscosity, g./(cm.)(sec.)
σ = $(D_G/D_L)^{1/2}$
τ = $\sigma\mathcal{H}/F$

Subscripts

A = of component A
AV = average
C = based upon concentration difference driving force
G = of the gas phase
L = of the liquid phase
m = average
o = initially
s = at the interface

Superscript

* = measured in the absence or suppression of resistance in the other phase; average value over entire interface

LITERATURE CITED

1. Acrivos, Andreas, *Chem. Eng. Sci.*, **9**, 242 (1958).
2. Beek, W. J., and C. A. P. Bakker, *Appl. Sci. Res.*, **A10**, 241 (1961).
3. Bird, R. B., W. E. Stewart, and E. N. Lightfoot, "Transport Phenomena," pp. 54-56, Wiley, New York (1960).
4. Butler, R. M., and A. C. Plewes, *Chem. Eng. Progr. Symp. Ser. No. 10*, **50**, 121 (1954).
5. Byers, C. H., and C. J. King, *U.S. Atomic Energy Comm. Rept. UCRL-16535* (1966).
6. Carslaw, H. S., and J. C. Jaeger, "Operational Methods in Applied Mathematics," p. 350, Dover, New York (1963).
7. Gilliland, E. R., and T. K. Sherwood, *Ind. Eng. Chem.*, **26**, 516 (1934).
8. Govindan, T. S., and J. A. Quinn, *AIChE J.*, **10**, 35 (1964). (1964).
9. Graetz, L., *Ann. Phys. Chim.*, **25**, 338 (1885).
10. Hatch, T. F., Jr., and R. L. Pigford, *Ind. Eng. Chem. Fundamentals*, **1**, 209 (1962).
11. Johnstone, H. F., and R. L. Pigford, *Trans. Am. Inst. Chem. Engrs.*, **38**, 25 (1942).
12. King, C. J., *AIChE J.*, **10**, 671 (1964).
13. ———, *Ind. Eng. Chem. Fundamentals*, **4**, 125 (1965).
14. Lapidus, Leon, "Digital Computation for Chemical Engineers," McGraw-Hill, New York (1962).
15. Lightfoot, E. N., *AIChE J.*, **8**, 416 (1962).
16. Nunge, R. J., and W. N. Gill, *Intern. J. Heat Mass Transfer*, **8**, 873 (1965).
17. ———————, *AIChE J.*, **12**, 279 (1966).
18. ———————, and R. P. Stein, *Ind. Eng. Chem. Fundamentals*, in press.
19. Shulman, H. L., C. F. Ullrich, A. Z. Proulx, and J. O. Zimmerman, *AIChE J.*, **1**, 253 (1955).
20. Stein, R. P., *ANL-6889* (Sept., 1964).
21. Tang, Y. P., and D. M. Himmelblau, *AIChE J.*, **9**, 630 (1963).
22. Vivian, J. E., and C. J. King, *ibid.*, **10**, 221 (1964).
23. Vivian, J. E., and D. W. Peaceman, *ibid.*, **2**, 437 (1956).

Manuscript received July 13, 1966; revision received August 15, 1966; paper accepted October 14, 1966. Paper presented at AIChE Detroit meeting.